2006

Tribological properties of quasicrystals: Effect of aperiodic versus periodic surface order

Jeong Young Park
Lawrence Berkeley National Laboratory

D. F. Ogletree
Lawrence Berkeley National Laboratory

M. Salmeron
Lawrence Berkeley National Laboratory

R. A. Ribeiro
Iowa State University

Paul C. Canfield
Iowa State University, canfield@ameslab.gov

See next page for additional authors

Tribological properties of quasicrystals: Effect of aperiodic versus periodic surface order

Abstract
We investigated the nanoscale tribological properties of a decagonal quasicrystal using a combination of atomic force microscopy and scanning tunneling microscopy in ultrahigh vacuum. This combination permitted a variety of in situ measurements, including atomic-scale structure, friction and adhesion force, tip-sample current, and topography. We found that thiol-passivated tips can be used for reproducible studies of the tip-quasicrystal contact while nonpassivated probes adhere irreversibly to the clean quasicrystalline surface causing permanent modifications. The most remarkable results were obtained on the twofold surface of the Al-Ni-Co decagonal quasicrystal where atoms are arranged periodically along the tenfold axis and aperiodically in the perpendicular direction. Strong friction anisotropy was observed on this surface, with high friction along the periodic direction and low friction in the aperiodic direction.

Keywords
Ames Laboratory, Materials Science and Engineering, Physics and Astronomy

Disciplines
Biological and Chemical Physics | Materials Science and Engineering | Physical Chemistry

Comments
This article is from *Physical Review B* 74, no. 2 (2006): 024203, doi:10.1103/PhysRevB.74.024203.

Authors
Jeong Young Park, D. F. Ogletree, M. Salmeron, R. A. Ribeiro, Paul C. Canfield, Cynthia J. Jenks, and Patricia A. Thiel

Tribological properties of quasicrystals: Effect of aperiodic versus periodic surface order

Jeong Young Park, D. F. Ogletree, and M. Salmeron*
Materials Sciences Division, Lawrence Berkeley National Laboratory, University of California, Berkeley, California 94720, USA

R. A. Ribeiro and P. C. Canfield
Ames Laboratory and Department of Physics and Astronomy, Iowa State University, Ames, Iowa 50011, USA

C. J. Jenks and P. A. Thiel
Ames Laboratory and Departments of Chemistry and of Materials Science and Engineering, Iowa State University, Ames, Iowa 50011, USA

(Received 4 April 2006; published 14 July 2006)

We investigated the nanoscale tribological properties of a decagonal quasicrystal using a combination of atomic force microscopy and scanning tunneling microscopy in ultrahigh vacuum. This combination permitted a variety of *in situ* measurements, including atomic-scale structure, friction and adhesion force, tip-sample current, and topography. We found that thiol-passivated tips can be used for reproducible studies of the tip-quasicrystal contact while nonpassivated probes adhere irreversibly to the clean quasicrystalline surface causing permanent modifications. The most remarkable results were obtained on the twofold surface of the Al-Ni-Co decagonal quasicrystal where atoms are arranged periodically along the tenfold axis and aperiodically in the perpendicular direction. Strong friction anisotropy was observed on this surface, with high friction along the periodic direction and low friction in the aperiodic direction.

DOI: 10.1103/PhysRevB.74.024203 PACS number(s): 46.55.+d, 61.44.Br, 68.37.Ps, 81.40.Pq

I. INTRODUCTION

Quasicrystals are metallic alloys exhibiting long-range atomic order but no translational periodicity.[1,2] About nine years after their discovery by Shechtman,[3] Dubois *et al.* reported that these materials exhibit anomalously low coefficients of friction when sliding against diamond and steel.[4] An explanation of this effect has been sought ever since. Understanding it is important in order to unravel the basic physics of friction and to facilitate practical applications. The most intriguing possibility is that the low friction is related to the exotic atomic structure of the bulk material.

The problem is still unresolved because two bodies in sliding contact constitute a very complex system. Until now, most experimental studies of tribology on quasicrystals[4–21]have been carried out under conditions in which irreversible (plastic) deformation takes place during sliding. Frictional energy dissipation measured under such conditions includes contributions from such diverse factors as the breaking of chemical bonds, generation of point defects, interactions with wear debris, phase transformations near the sliding track, and in crystalline materials by creation of dislocations and propagation of slip planes in specific crystallographic directions. Some of these factors have been proposed to play a role in the observed low friction coefficients of quasicrystals. Although these phenomena are important in practical situations, they obscure the fundamental relationship between friction and atomic scale structure. Plastic deformation must be avoided if the goal is to explore this relationship, as it is in the present work.

In the regime of "wearless" friction, no irreversible changes such as broken chemical bonds or permanently displaced atoms occur at either of the surfaces in contact. If the contact between the two sliding bodies is such that only reversible (elastic) deformations take place, energy dissipation occurs through the generation of vibrational or electronic excitations near the contact. These excitations propagate into the bulk solid and thermalize, converting kinetic energy into heat. Here we report on a significant anisotropy in friction when an atomic force microscope (AFM) tip slides along the periodic or aperiodic directions of the twofold decagonal quasicrystal surface. We conclude that this anisotropy may contribute to the low friction observed in macroscopic measurements on quasicrystals, although its importance (relative to wear, bulk deformation, etc.) in real applications will undoubtedly depend upon the conditions of sliding.

The atomic structure of a quasicrystal surface cannot be studied in air because of the presence of an oxide film, making ultrahigh vacuum a necessary environment. A set of studies in ultrahigh vacuum has been reported by Gellman *et al.*,[8,10,11] who found that the friction coefficient of clean, single-grain quasicrystalline Al-Pd-Mn is half that of a crystalline Al-Pd-Mn alloy with similar stoichiometry. However, they found no variation in friction coefficient across a series of quasicrystalline-related phases in the Al-Cu-Fe family, leading them to suggest that friction is not related to atomic structure.[15] Since these measurements were made under conditions of plastic deformation, it is not clear how such deformation changes the structure of the sliding interface.

The dual objective of using a clean surface, yet only deforming the surface reversibly, is not achieved easily. Previous work has shown that adhesive forces between clean metals are very strong, as expected, making irreversible deformations unavoidable.[22] Specifically, with W_2C-coated AFM tips, pull-off forces as large as 1.0 μN with a tenfold Al-Ni-Co quasicrystal surface[13,23] and 16 μN with Pt (111) (Ref. 22) have been measured. This large adhesion produced damage to the quasicrystal surface as a result of rupture of the strong chemical bonds formed upon contact. One practical way to avoid damage is to passivate either surface or tip.

We previously reported a passivation strategy consisting of ethylene chemisorption on the quasicrystal surface, which allowed us to probe adhesion and friction either in the elastic or inelastic regime, depending on applied load.[14] The disadvantage of this strategy is that the saturated layer of ethylene reacts chemically with the surface, perturbing the atomic structure.

In this study, we passivate the probe instead of the substrate by coating the conductive tip with alkanethiol molecules. In this way, we can preserve the quasicrystal surface and directly investigate the correlation between its atomic structure and tribological properties. (A similar approach to measuring friction, using a thin film transferred to the apex of an AFM probe, has been reported by other authors.[24,25]) We chose the twofold surface of the decagonal Al-Ni-Co phase, since it presents both periodic and aperiodic atomic arrangements in the same surface, allowing *in situ* comparisons of friction along crystalline and quasicrystalline directions. A short report of friction anisotropy on this surface,[26] as well as an analysis of the surface structure, have been published elsewhere.[27]

II. EXPERIMENTAL DESCRIPTION

The samples were prepared and characterized in an ultrahigh vacuum (UHV) chamber with a base pressure of 1.0×10^{-10} Torr. The chamber contained a commercial RHK microscope mounted on a 6-in. flange.[28] The sample could be translated from the microscope to a three-axis manipulator with a heating stage. Cleaning was accomplished by a combination of electron beam heating and Ar^+ ion sputtering. Low-energy electron diffraction (LEED) and Auger electron spectroscopy (AES) were used for surface analysis. Samples and cantilevers could also be introduced through a load-lock without breaking vacuum, which made possible measurements using cantilevers with different spring constants and metal coatings.

Two operation modes were possible in our apparatus: AFM and STM (scanning tunnelling microscopy). By using conductive cantilevers, the electrical current between tip and sample, normal force (lever bending), and friction force (lever twisting) could be measured. In STM mode, the tunneling current was used for feedback, while the bending of the cantilever could be measured simultaneously. This was useful to monitor the variation of force during STM imaging.[29,30] In contact AFM mode, the normal force was used for feedback, which yielded topography, while friction force and current were measured simultaneously.

Two types of cantilevers coated with about 50 nm of either W_2C or TiN, and with spring constants of 48 N/m for STM and 2.5 N/m for contact AFM, were used.[31] While the stiff cantilevers suppressed the jump to contact instability, ensuring stable tunneling in STM mode, the soft cantilevers allowed higher force sensitivity.

To determine forces, the cantilever spring constant was calibrated using the method of Sader *et al.*[32] while the lateral force was calibrated with the method of Ogletree *et al.*[33] The radii of the metal-coated tips were 30–50 nm before contact, as measured by scanning electron microscopy. When measured after a contact experiment, however, the radii were found to be 80–120 nm. Since the measured friction force did not change at constant load and did not show time-dependent behavior in the elastic regime, we assume that the changes in tip radius took place soon after the first contact, with minimum changes during subsequent contact measurements.

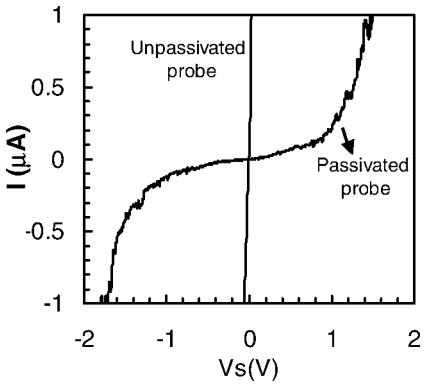

FIG. 1. Current vs voltage curves between a TiN tip and atomically clean Al-Ni-Co twofold surface at an applied load of 50 nN. They illustrate the metallic vs semiconducting nature of the interface for an unpassivated and an alkylthiol-passivated tip.

The AFM tip was coated with a C_{16} alkanethiol in UHV. In order to do this, a sacrificial Au substrate covered with a partial monolayer of alkanethiol was inserted in the UHV chamber.[34] The tip was scanned over this Au surface at a load of 50–100 nN. Changes in the distribution of the alkanethiol on the Au surface were visible during scanning, and were accompanied by transfer of molecules to the tip. This was confirmed by measuring the conductance of the tip in contact with regions of bare Au. The change in the electrical nature of the contact is shown in Fig. 1, which shows the current versus sample bias of passivated and nonpassivated probes at an applied load of 50 nN. Before passivation, the linearity of the curve indicated metallic or Ohmic behavior. After passivation, the shape of the curve indicated nonmetallic behavior. Also, the conductance (dI/dV) of the junction changed. The conductance at 1 V bias was 10^4 times smaller after passivation. This change in conductance was a reliable indicator of tip passivation. Reported values of the friction force or current in this study were obtained by averaging over the area covered by an image.

The sample had dimensions of $1\ \text{cm} \times 1\ \text{cm} \times 1.5$ mm and was cut from a large single grain $Al_{72}Ni_{11}Co_{17}$ quasicrystal grown at the Ames Laboratory, in Iowa State University.[35] The chemical composition was determined by energy-dispersive x-ray analysis in a scanning electron microscope. After degreasing by ultrasonic agitation in acetone and methyl alcohol, the sample was introduced in the UHV chamber. The *in situ* cleaning process consisted of cycles of Ar^+ ion sputtering with 1 keV ion energy followed by heating for 1–2 h at a temperature up to 1150 K, as monitored by an optical pyrometer (Minolta Land) using an emissivity of 0.35.[36] This produced a clean and ordered sample, as judged by LEED and Auger electron spectroscopy.

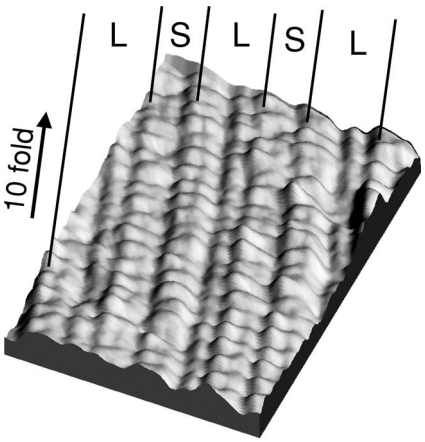

FIG. 2. Atomically resolved STM image (50×75 nm) of the Al-Ni-Co twofold surface. Tunneling bias and current are +1.5 V and 0.2 nA. Atomic rows separated by long and short distances (L,S) are marked by lines.

III. RESULTS AND MODELING

A. Atomic structure of the twofold Al-Ni-Co decagonal quasicrystal

In Fig. 2, we show an atomically resolved STM image of the twofold surface revealing the presence of atomic rows along the tenfold direction with an internal periodicity of 0.4 nm. Hence, the tenfold axis is the periodic direction, as expected from the bulk structure.[37] Along the orthogonal axis in the surface plane, the spacing between the rows follows a Fibonacci sequence with inflation symmetry. The details of the atomic structure of this twofold Al-Ni-Co surface are presented elsewhere.[27] The majority of the terraces display this type of structure, under the conditions of preparation used here.

B. Elastic and plastic contacts

In a previous study, we reported results of contacts using the tenfold surface of a decagonal Al-Ni-Co quasicrystal and a TiN-coated tip, also separated by a layer of molecules.[14] In that case the molecule, ethylene, was adsorbed on the quasicrystal surface instead of the tip. We showed that elastic contact occurred at low loads, and that an abrupt transition to irreversible deformation occurred at pressures above 3.8–4.0 GPa.[14] In the present study, the surface symmetry (twofold versus tenfold) and the chemical nature of the organic molecules (alkylthiols versus ethylene) are different, but the two regimes can still be accessed at different loads.

The adhesion force was measured by means of approach and retraction curves. Figure 3(a) shows results at a bias voltage of 0 V. For the passivated tip, the adhesion force was 180±50 nN, lower than that obtained with the nonpassivated probe by a factor of 2. The adhesion force as a function of applied load is shown in Fig. 3(b). As can be seen, the adhesion force for passivated tips remained low when the maximum applied load was below 200 nN, and was about two times higher for higher peak loads. The value of the adhesion force above the threshold is similar to that obtained

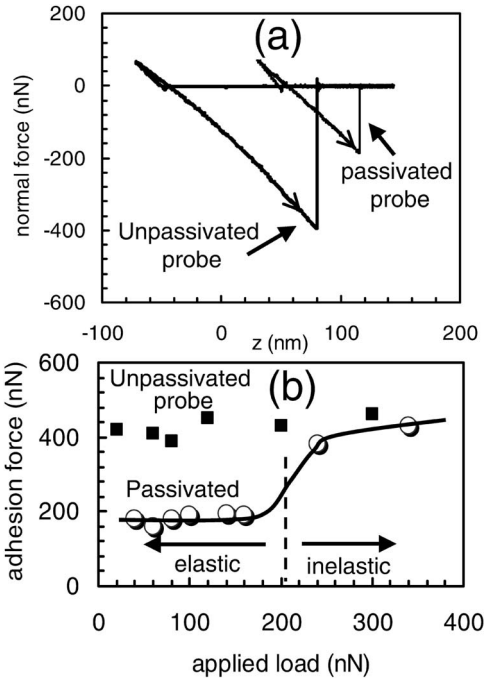

FIG. 3. (a) Force-distance curves at 0 V bias, for passivated and unpassivated tips. The tip was coated with TiN (spring constant 2.5 N/m) and the surface was the clean twofold Al-Ni-Co surface. (b) Adhesion force as a function of peak applied load, at a sample bias of 0 V measured on the twofold Al-Ni-Co decagonal surface. Open circles represent data for the passivated tip, and closed squares the unpassivated tip.

with a nonpassivated tip at any applied load. The total contact force at the threshold for loss of tip passivation was 380 nN after adding the adhesion force (180 nN).

The friction at a nanometer-scale contact can often be described as the product of the real tip-sample contact area and a material-dependent shear stress.[38] In this model, the shear stress is independent of applied load, and the observed variation of friction with load is due to changes in the contact area. The relation between contact area and applied load can be described by the Derjaguin-Muller-Toporov (DMT)[14,39,40] or the Johnson-Kendall-Roberts (JKR)[41] models, depending on the adhesion force and hardness of the sample. Generally, the JKR model is appropriate for soft materials with large adhesion, while DMT applies best in the case of high stiffness and low adhesion. As we will show, the friction data using passivated tips show good agreement with the DMT model, consistent with the high hardness of the quasicrystal and coating materials (TiN). Hence, the DMT model was used to calculate the contact area.[40,42]

In the this model, the friction force (F_f) is

$$F_f = \tau A = \tau\left[\pi\left(\frac{R^{2/3}}{K^{2/3}}\right)(L + L_c)^{2/3}\right], \quad (1)$$

where A is the contact area, τ is the shear stress, R is the tip radius, L_c is the adhesion force, and K is the combined elastic modulus of the two materials, given by $K=4/3[(1-v_1^2)/E_1+(1-v_2^2)/E_2]^{-1}$, where E_1 and E_2 and v_1 and v_2 are

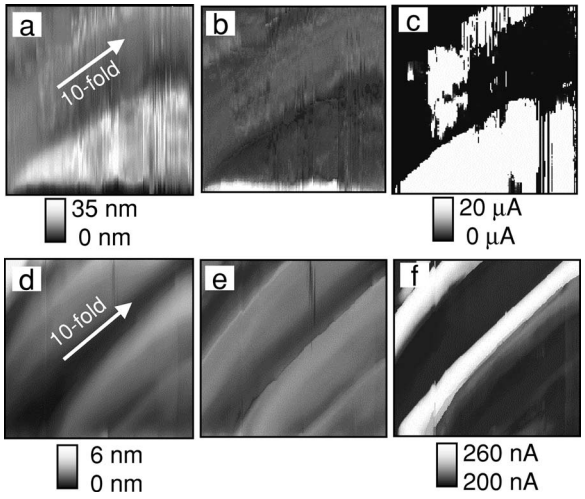

FIG. 4. AFM contact mode images, 500 nm×500 nm. (a) Topography, (b) friction, and (c) current acquired simultaneously in the plastic regime with an unpassivated probe (bare metal coated tip) revealing unstable and irreversible features. Applied load=0 nN, and sample bias=0.1 V. (d) Topography, (e) friction, and (f) current in the elastic regime measured with a passivated probe. Applied load=0 nN, and sample bias=1.5 V. Fast scanning was in the vertical direction. Features characteristic of the tip sticking to the surface at the start of the scan lines are visible at the bottom of the images.

the Young modulus and Poisson ratios, respectively. Using L_c=180 nN, R=100 nm, and a combined elastic modulus (K) of 171 GPa (E_{TiN}=600 GPa, E_{QC}=200 GPa,[20] ν_{TiN}=0.25,ν_{QC}=0.38), we find A=115 nm^2. The P (pressure) corresponding to the threshold load is then easily calculated as F_n (the effective applied load)/A=380 nN/115 nm^2 =3.3 GPa.

Attempts at imaging the clean surface with a nonpassivated interface proved unsuccessful and led to irreversible modifications. An example is shown in Figs. 4(a)–4(c), where the topography, friction, and current images show discontinuous line scans associated with the formation and rupture of chemical bonds. The tip-sample current is particularly affected by the nature of the tip-sample mechanical contact, and for that reason it is very unstable in this inelastic regime. The instabilities in the images disappear after tip passivation. Figures 4(d)–4(f) show reproducible topographic, friction, and current images acquired with such tips.

Reversibility was also checked by comparing zoomed-out low-load images before and after friction measurements. No irreversible changes such as wear tracks or mounds of displaced material at the edges of the high-load scan area were observed.

C. Modeling cantilever deformations due to friction forces

The unique symmetry of the twofold decagonal quasicrystal surface, with quasiperiodic atomic structure along the twofold axis and periodic structure perpendicular to this axis, allowed us to investigate the effect of order on wearless friction. We performed a series of experiments to explore friction anisotropy as a function of scanning direction. In a conventional scanning force microscope, friction is measured by scanning the tip along the surface perpendicular to the cantilever axis. The torsional response of the cantilever is then proportional to tip-sample friction, and the normal load applied to the tip-sample contact is not affected by friction. In an optical deflection SFM, a laser beam reflected off the cantilever surface close to the tip measures changes in the cantilever slope. Torsional and normal slope changes are proportional to frictional and normal forces acting on the tip. Rotating the scan angle relative to the cantilever axis introduces complications, since frictional forces now modulate the normal load applied to the contact, and the optical deflection signals show a mixed response to normal and frictional forces.

Friction anisotropy has been investigated on self-assembled molecular films in ambient conditions by macroscopically rotating the sample substrate, relocating the region of interest, and acquiring friction data for different scan directions using the conventional AFM geometry.[43–45] Special purpose ultrahigh-vacuum AFM instruments have been constructed to allow friction anisotropy to be explored directly.[24] This approach was not possible in our ultrahigh-vacuum AFM. We measured the friction force of the clean twofold Al-Ni-Co surface against alkylthiol-passivated TiN tips by changing the scanning direction of the AFM tip while holding the sample in a fixed position. We explored friction anisotropy on the twofold quasicrystal surface by orienting the sample such that the AFM cantilever axis was 45° away from the twofold symmetry axis. In this orientation, we could scan the tip along either the periodic or quasiperiodic directions and obtain the same instrumental response. We observed a significant friction anisotropy, which is discussed below. Before presenting these data, we first analyze the instrumental response of the AFM to scan direction. This analysis was verified by angle-dependent friction experiments performed on isotropic surfaces.

The scanning direction was defined by the angle θ with respect to the short axis of the cantilever, as illustrated in Fig. 5(a). In the conventional AFM geometry with θ=0°, friction force causes the lever to twist around its long axis, producing a torsional response signal. When $\theta \neq 0°$, the torsional response is reduced by $\cos(\theta)$ since only a component of the friction force creates a torsional response. Another component of friction acts along the lever axis. Since the lever axis is tilted relative to the surface plane, a force along the lever axis changes the effective normal load applied to the contact, as shown in Fig. 5(b). Consider the cantilever as a rigid object free to pivot around its base. A force in the sample plane, shown by the horizontal arrow, can be resolved into a component along the line connecting the tip apex to the lever base, which tends to buckle the lever, and a perpendicular component, which tends to deflect the lever. Since the stiffness of the tip-sample contact is much larger than the lever spring constant, the tip is constrained to move in the sample plane.

The cantilevers used in our experiments had tip height H=15 μm and lever length L=200 μm, so a line from the base of the cantilever through the tip apex is tilted relative to the lever by $\arctan(H/L)$=4.3°. In our AFM, the lever is tilted by 22.5° from the vertical for a total tilt angle α

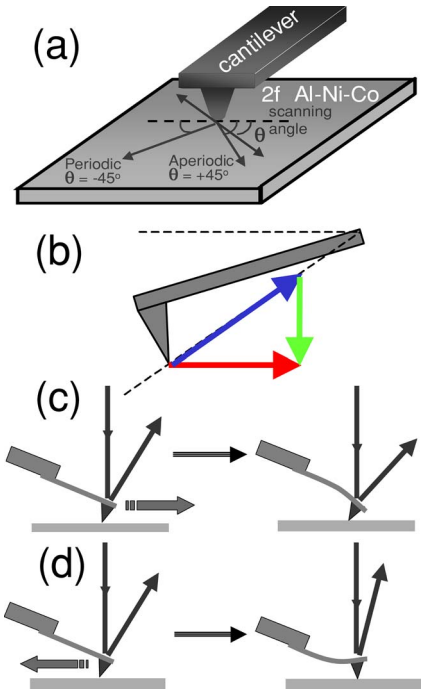

FIG. 5. (Color online) (a) Schematic of the rotational scanning of the AFM head used to investigate the friction anisotropy on the twofold decagonal quasicrystal. (b) A force F_x (red arrow) in the sample plane acting along the lever axis can be resolved into a "buckling" component along the line connecting the tip apex to the lever base (blue arrow), and a component normal to the sample surface marked by the green (light gray) arrow. Friction forces along the lever axis modulate the normal load. (c,d) Effect of buckling forces on the measured normal force (deflection response). In (c), the tip experiences a frictional force while scanning in the direction indicated by the gray arrow. The response of the lever resolves a component of the friction force normal to the surface, *increasing* the effective load, and a component along the lever, buckling the cantilever and *decreasing* the deflection signal. In (d), the scanning direction is reversed, and the friction force *reduces* the effective load and *increases* the deflection signal. These changes in effective load in turn modify the friction and the lever torsional response.

$=22.5°+4.3°=26.8°$. Therefore, a friction force component acting on the tip in the sample plane and along the lever axis F_x modulates the externally applied load by $\Delta F_z=-\tan(\alpha)$ $F_x=-0.51F_x$, and also results in a lever "buckling" force $F_b=F_x/\cos(\alpha)=-1.12F_x$. Here the positive x direction points from the base of the lever toward the tip. The linear "contact lines" in the force-distance curves of Fig. 3(a) confirm that the stiffness of the tip-sample contact is large compared to that of the lever. From the DMT model parameters used in Eq. (1), the contact stiffness should be about 1600 N/m at zero external load, much greater than the cantilever stiffness of 2.5 N/m.

When $F_x=0$, the deflection response of the cantilever increases in proportion to the deflection Δz of the tip apex. At a given value Δz, changes in F_x will also change the shape of the cantilever beam and the deflection signal, as shown in Figs. 5(c) and 5(d). A positive force F_x will *reduce* the tip-sample load and *increase* the deflection signal. If the AFM feedback is active, the control loop will pull the cantilever away from the surface, further reducing the effective tip-sample load. Likewise, a negative F_x *increases* the tip-sample load while *reducing* the deflection signal, leading the feedback loop to further increase the applied force. In fact, if the friction and the lever tilt angle α are sufficiently high, the AFM feedback becomes unstable, and the lever height will oscillate. To avoid this complication, our scan-direction-dependent friction measurements were carried out in open loop, i.e., with the feedback control disabled. The AFM x-y scanning plane was first adjusted to be parallel to the sample surface, so that the applied force for $F_x=0$ remained approximately constant.

The effect of frictional anisotropy is calculated as follows. We assume that the friction force $f(L,\theta)$ is a function of applied load and scanning direction. We further assume, for simplicity, that the load dependence is separated from the angular dependence, which is an elliptical function, with anisotropy β (ratio of maximum to minimum friction for a given load). Then the anisotropic friction is given by

$$f(L,\theta)=g(L)h(\theta), \tag{2}$$

$$h(\theta)=\frac{1}{\sqrt{\cos^2(\theta-\phi)+\beta^2\sin^2(\theta-\phi)}}, \tag{3}$$

where $g(L)$ includes the dependence of friction on applied load and $h(\theta)$ describes the anisotropy. Different assumptions about anisotropy change the form of $h(\theta)$. The effect of forces F_x acting along the lever can be taken into account by expanding $g(L_0+\Delta L)=g_0+\mu_1\Delta L+\cdots$ around the externally applied load L_0. F_x modulates the externally applied load by $\Delta F_z=-\tan(\alpha)$ $F_x=-0.51F_x$. As a function of scan angle θ, the effective load is changed by

$$\begin{aligned}\Delta L&=\tan(\alpha)\sin(\theta)f(L,\theta)=\tan(\alpha)\sin(\theta)h(\theta)(g_o+\mu_1\Delta L)\\&=\gamma(g_o+\mu_1\Delta L),\end{aligned} \tag{4}$$

$$\Delta L=\frac{\gamma g_o}{1-\gamma\mu_1}, \tag{5}$$

where the $\sin(\theta)$ term gives the component of frictional force in the x direction and γ groups the angular terms. Finally, the corrected frictional force is

$$f(L_0+\Delta L,\theta)=\left[g_o+\left(\frac{\mu_1\gamma g_o}{1-\gamma\mu_1}\right)h(\theta)\right]=\frac{g_o h(\theta)}{1-\gamma\mu_1} \tag{6}$$

and the torsional response $\mathrm{TR}(\theta)$ of the cantilever is proportional to the component of friction acting perpendicular to the cantilever, i.e., the above expression multiplied by $\cos(\theta)$ or

$$\mathrm{TR}(\theta)=\frac{g_o\cos(\theta)h(\theta)}{1-\mu_1\tan(\alpha)\sin(\theta)h(\theta)}. \tag{7}$$

Predictions of this model are shown in Fig. 6 for the forward and reverse scan directions. The torsional response is normalized to g_0, the peak friction at load L_0, for an anisotropy direction (direction of maximum friction) $\phi=-45°$. The

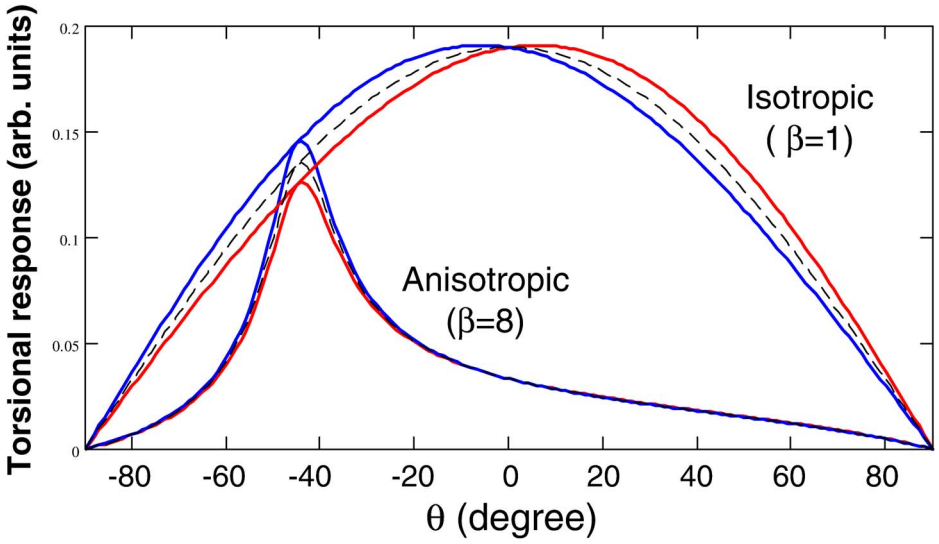

FIG. 6. (Color online) Calculated torsional response for an isotropic surface ($\beta=1$) and for an anisotropic surface with $\beta=8$ and $\phi=-45°$ for a friction coefficient $\mu_1=0.19$ as a function of scanning angle. The red lines show the "trace" and the blue lines the "retrace" response calculated with Eq. (7). The dashed black lines show the uncorrected response from Eqs. (2) and (3). Although lever effects modulate the friction by about 15%, these effects cancel out to first order when trace and retrace are averaged.

slope of the friction-load curves was set to $\mu_1=0.19$, the experimental value for the quasicrystal surface at zero external load. Two pairs of curves are shown for the cases $\beta=1$ (no anisotropy) and $\beta=8$. The solid lines include the friction/load correction, which is about ±10%. When the friction responses for trace and retrace are averaged (half the width of the friction loop) as is commonly done experimentally, the corrections cancel to first order, and the residual effect of the force correction is only 0.5%.

The model was verified by comparing simulation results with experimental data for an isotropic amorphous silicon oxide surface, having a root-mean-square roughness of 2.5±0.6 Å. The surface topography is shown in Fig. 7(a). The silicon oxide was prepared with a wet chemical method,[46] leading to a chemically inert oxide layer with a thickness of 3.7±0.5 Å.[47] The squares in Fig. 7(b) show the measured torsional response of the lever as a function of θ. It decreases as θ deviates from zero, as expected. The agreement between the experimental data and the simulation (solid line) is excellent, supporting the validity of our model.

D. Friction anisotropy on the twofold decagonal quasicrystal surface

We found that the torsional response of the contact between the twofold Al-Ni-Co decagonal quasicrystal surface and the alkylthiol-passivated TiN probe was highly anisotropic. The torsional response was high along the tenfold (periodic) direction, and low along the twofold (aperiodic) direction. Figure 8 shows the torsional response as a function of applied load measured along both the periodic direction and the aperiodic directions. As shown in Fig. 8, the adhesion force obtained from force-distance curves while scanning in different directions produced the same value ($\sim$130 nN) for both periodic and aperiodic directions, as expected. In this experiment, the sample was oriented with the tenfold and twofold axes at $\theta=\pm45°$. By symmetry, the magnitude of the coupling between the twisting and buckling of the cantilever should be equal at these two angles. The lines through the data are fits to the DMT equations for elastic contact area and constant contact shear stress, which as can be seen agree quite well with the data. Because the DMT is appropriate for hard and poorly adhesive interfaces,[48] the good fits of Fig. 8 reflect the high elastic modulus of both tip (TiN) and sample (quasicrystal), and the reduced adhesion that is the result of the tip passivation by the alkanethiol. The top curve, labeled "friction anisotropy," is simply the ratio of the lower two. As the curve shows, the anisotropy does not depend on applied load, over a range of −130 to +70 nN, and has a value of 8.2±0.4. These fits give a shear stress of

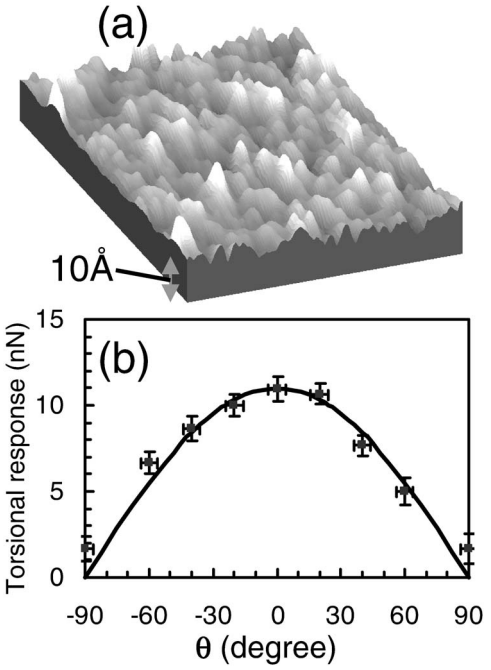

FIG. 7. (a) AFM image (500 nm×500 nm) of a silicon oxide surface with a roughness of 2–3 Å. (b) Plot of torsional response measured as a function of scanning angle in open loop, along with the predictions (continuous curve) of our friction model (see text) describing the coupling between cantilever twist and buckling deformations.

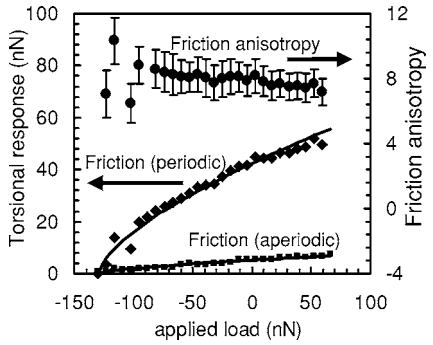

FIG. 8. Torsional response as a function of applied load for periodic and aperiodic directions, showing a friction anisotropy ratio of ~8. The adhesion force is 130 nN. The lines are fits to the DMT model for contact shear stresses of 690 and 85 MPa.

690 MPa in the periodic direction and 85 MPa in the aperodic direction.

Figure 9(a) shows the torsional response of the cantilever as a function of scanning direction at an applied load of 0 nN. The overlaid curve shows the calculated torsional response as a function of rotation angle assuming an elliptical friction anisotropy ratio of 8, consistent with the measured variation of the friction in the previous experiment. In Fig. 9(a), we also show the current measured simultaneously with the torsional response. In the elastic regime, conductance is a convenient way to ensure constancy of the contact area. The conductance is constant within 5%, indicating that the contact area is invariant with scanning angle. The data points in Fig. 9(b) show the effective friction force obtained from the measured torsional response after normalizing by the geometrical factor associated with skewed scanning. Clearly the friction force reaches a maximum at an angle of −45° and a minimum at +45°.

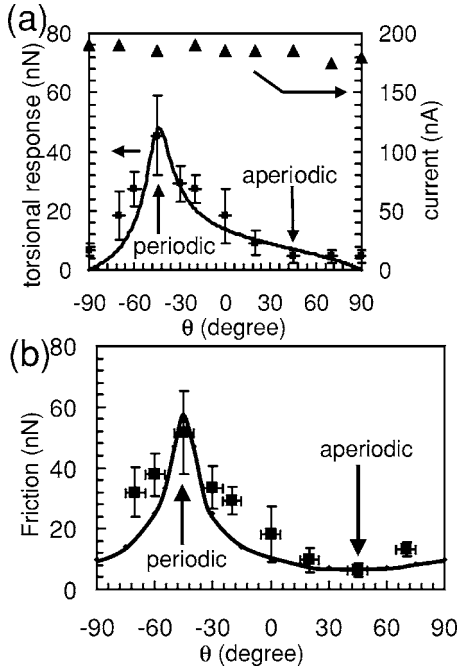

FIG. 9. (a) Torsional response of the cantilever measured as a function of scanning angle on the twofold surface of the Al-Ni-Co decagonal quasicrystal at zero external load. The torsional response was higher along the periodic direction than along the aperiodic direction. The solid line shows the calculated torsional response with scanning angle for an elliptical anisotropy factor (ratio of torsional response) of 8. Current at the sample bias of 1.0 V was measured at the same time as torsional response. Its constancy reflects the elastic tip-sample contact, and the fact that uniformity of the applied load is within 5%. (b) Effective friction forces (torsional response after compensation for rotational scanning) as a function of the scanning angle. The solid line shows the calculated friction force after inclusion of a friction anisotropy value of 8. The exact shape of the calculated friction force is associated with the elliptical anisotropic model described in the text.

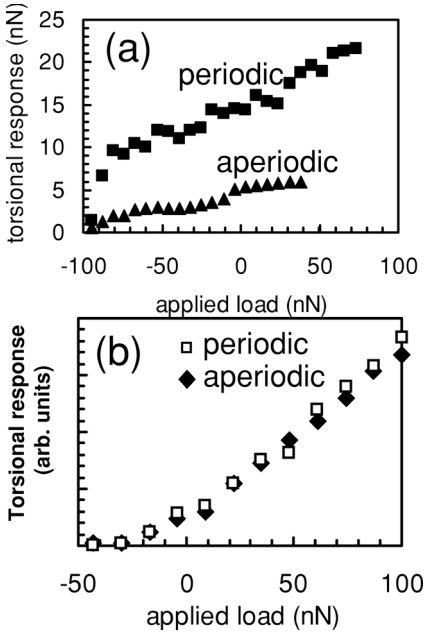

FIG. 10. (Color online) (a) Torsional response vs applied load measured with the molecule-passivated AFM probe after exposing the surface to 100 L ethylene. (b) Torsional response vs applied load on the air-oxidized quasicrystal surface after "long air oxidation" as described in text.

E. Friction anisotropy after surface modifications

The torsional anisotropy discussed in the previous section could be influenced by surface modifications. For example, we found that the friction anisotropy measured with passivated AFM probe dropped by half to 3 to 4 after exposing the surface to 100 L of ethylene gas, as shown in Fig. 10(a). In this experiment, ethylene exposure was performed by backfilling the chamber to a pressure of 4.0×10^{-7} Torr at room temperature. No ordered structures were formed on this surface as shown by LEED.[14] The decrease in the friction anisotropy suggests that the anisotropy of the clean surface arises from short-range interactions between tip and surface.

In a different experiment we found that the friction anisotropy disappeared completely when the surface was oxidized by exposure to air. Figure 10(b) shows the torsional response measured on a surface oxidized by several months exposure to air.[23] Extrapolating from studies of icosahedral Al-rich

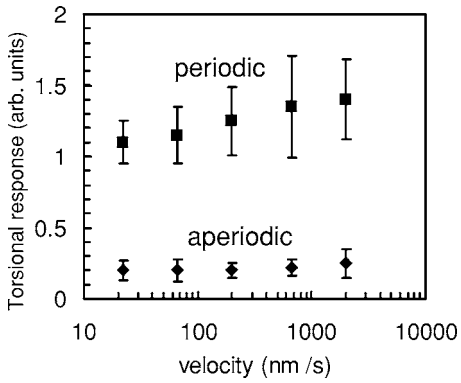

FIG. 11. Torsional response as a function of the scanning speed measured in periodic and aperiodic directions.

quasicrystals,[49,50] exposure to air at room temperature should form a surface layer of nearly pure aluminum oxide, 2–3 nm thick. The thicker oxide layer is more effective at screening the interaction responsible for the anisotropy than the ethylene monolayer.

F. Velocity dependence

The velocity dependence of the torsional response might help elucidate the mechanisms of energy dissipation. Figure 11 shows the measured velocity dependence of the torsional response in both the periodic and aperiodic directions. While torsional response in the aperiodic direction shows little dependence on velocity, that in the periodic direction increases by 20% with increasing velocity. Unfortunately the error bars are quite large at high scanning speed and prevent us from concluding whether the dependence is linear.

IV. DISCUSSION

Any explanation for the observed friction anisotropy must describe an anisotropy in the rate at which kinetic energy is dissipated at the sliding interface. Several types of explanations can be considered.

At constant load and fixed geometry, the area of a single contact is controlled by hardness, in the plastic regime, and by Young's modulus in the elastic regime. Indeed, it has been speculated that the low coefficient of friction of quasicrystals, relative to other materials, is due in part or in total to their high hardness.[11] In the present experiments, the frictional anisotropy was measured under conditions in which the contact area was constant as a function of the rotational angle. This is expected, based on the constant applied load and the elastic nature of the contact. This is confirmed by the observed invariance in the conductance, which is independent of θ to within 5%. Hence, we can eliminate changes in contact area with scanning direction as an explanation for our data.

Friction anisotropy on Ni(100) has been observed under conditions of plastic deformation, and ascribed to easy shearing along preferred slip planes in the bulk.[51] This explanation does not apply to our data due to the absence of plastic deformation.

Another potential explanation involves the hexadecanethiol molecules that coat the tip and their response to the surface corrugation (Fig. 2). The hydrocarbon chains might be relatively confined as the tip sweeps along the channels, but be forced to move more erratically when the tip scans perpendicular to the rows. A simple analogy might be to a broom sweeping along a corrugated surface. However, the length scales do not support this explanation: The peak-to-peak surface corrugations along periodic and aperiodic directions differ only slightly (0.03 nm versus 0.04 nm peak-to-peak),[27] and are very small compared with the size of the alkyl chains, which are 0.4 nm in diameter and 2 nm long. Note that the corrugation between rows in Fig. 2 is enhanced due to electronic effects.[27] Furthermore, in the broom analogy, sweeping is expected to be easiest parallel to the direction of corrugation, which is opposite to our experimental observation.

Recently, Dubois *et al.* have shown that the friction coefficients of quasicrystals and related materials correlate well with the reversible adhesion energy of water[7] and suggested that the two phenomena share a common origin in the electronic structure of the material. Since in our case the friction anisotropy was measured on a single surface, the adhesion energy between the tip and the quasicrystal is constant. That is to say, the adhesion force is the force needed to rupture the interface by moving the tip along the surface normal, which does not have a component in the surface plane and hence cannot contribute to the surface anisotropy.

Several observations of friction anisotropy in elastic and reversible contacts have been attributed to the degree of registry (commensurability) between two solids as a function of sliding angle.[24,52–55] Efficient energy dissipation through phonon generation normally requires atomic-scale instabilities, where atoms suddenly "jump" or "slip" from metastable to stable configurations. In the case of wearless friction, the forces between atoms across the contact are normally relatively weak compared to the interatomic forces within each solid. If this is not the case, then irreversible contacts with plastic deformation and atom transfer are likely, as we see for unpassivated contacts between an AFM tip and a clean quasicrystal surface. These weak forces normally result in gradual, adiabatic displacements of contact atoms from their equilibrium positions and little phonon generation. Even weak interaction potentials, however, can exhibit nonadiabatic "stick-slip" behavior for periodic contacts, while incommensurability inhibits phonon excitation at the sliding interface, and hence can lead to low friction forces.[56] Ever since low friction was first discovered in quasicrystals, incommensurability has been considered as a possible cause.[57] In our experiments, however, the TiN tip is of a different material and probably amorphous, and hence should be incommensurate in both periodic and aperiodic directions. Registry is therefore unlikely in any scanning direction. However, periodic stick-slip has frequently been reported for AFM contacts between a periodic surface and an amorphous tip. The twofold decagonal quasicrystal surface does allow us the unique opportunity to slide the same tip across a chemically identical surface, changing the degree of order by changing direction. The observation of a significant friction anisotropy adds weight to the notion that order plays a significant role in wearless friction.

The thermal and electrical conductivities of quasicrystals are notably low relative to typical metals.[58–60] This leads to a high degree of anisotropy in bulk electrical and thermal conductivity in the decagonal phases.[61] The transport properties are "normal" along the periodic direction, but anomalous in the aperiodic ones in the decagonal phases. For instance, the bulk thermal conductivity is larger along the periodic direction than along the twofold direction by an order of magnitude at room temperature in Al-Ni-Co. The low thermal conductivity of quasicrystals is attributed to the fact that the density of free electrons is low, so that heat propagates mostly by atomic vibrations. The observed anisotropy, however, is not likely to be related to the heat dissipation, via electron or thermal conductivity, after its generation during rubbing. It could originate in some anisotropy in the excitation mechanism, most likely phonon excitation.

Phonons do not travel easily in a lattice when their wavelength is comparable to the size of the atoms or clusters of atoms, and that gives rise to band gaps in the spectrum. Theoretical calculations of the phonon energy spectrum have shown that additional gaps are developed in the aperiodic directions when the spring constant associated with atomic arrangements is also aperiodic.[62,63] This could explain our observations because the tip motion tends to excite vibrations along the direction of its motion and the presence of gaps would make excitation of such phonons less efficient.

A quantitative analysis of friction in relation to the electrical and heat transport properties is intriguing and worthy of further theoretical investigation. Understanding such a relationship may bring new insights into the most fundamental aspects of tribology, and in particular of quasiperiodic and periodic structures.

V. CONCLUSION

In conclusion, using a specially cut decagonal quasicrystal that produced a surface parallel to the decagonal axis, we have shown that there is a strong anisotropy in the friction properties related to the existence or not of periodicity. High friction is found along the periodic direction and low friction along the aperiodic direction. We have shown also how angle-dependent friction properties can be studied using standard AFM cantilevers by separating the twisting and buckling contributions. We have shown the mathematical expressions that describe the coupling between these two deformation modes.

We have shown that the passivation of our TiN tip probe allowed us to obtain stable, reversible, elastic contacts with the atomically clean quasicrystal surface. We showed that the anomalously low friction force in the aperiodic direction is associated with the exotic atomic structure of the quasicrystal.

ACKNOWLEDGMENTS

This work was supported by the Director, Office of Energy Research, Office of Basic Energy Sciences, Materials Sciences Division, of the U.S. Department of Energy through the Ames Laboratory, Contract No. W-405-Eng-82, and through the Lawrence Berkeley National Laboratory, Contract No. DE-AC02-05CH11231.

*Author to whom all correspondence should be addressed. Electronic address: mbsalmeron@lbl.gov

[1] C. Janot, *Quasicrystals: A Primer* (Clarendon Press, Oxford, 1992).
[2] J.-M. Dubois, *Useful Quasicrystals* (World Scientific, New Jersey, 2005).
[3] D. Shechtman, I. Blech, D. Gratias, and J. W. Cahn, Phys. Rev. Lett. **53**, 1951 (1984).
[4] J. M. Dubois, S. S. Kang, and J. Vonstebut, J. Mater. Sci. Lett. **10**, 537 (1991).
[5] C. Dong, L.-M. Zhang, Q.-G. Zhou, H.-C. Zhang, J.-M. Dubois, Q.-H. Zhang, Y.-C. Fu, F.-Z. He, and F. Ge, Bull. Mater. Sci. **22**, 465 (1999).
[6] J.-M. Dubois, P. Brunet, W. Costin, and A. Merstallinger, J. Non-Cryst. Solids **334-335**, 475 (2003).
[7] J. M. Dubois, V. Fournée, and E. Belin-Ferré, in *Quasicrystals 2003—Preparation, Properties and Applications*, edited by E. Belin-Ferré, M. Feuerbacher, Y. Ishii, and D. J. Sordelet (MRS, Warrendale, PA, 2004), pp. 287–298.
[8] J. S. Ko, A. J. Gellman, T. A. Lograsso, C. J. Jenks, and P. A. Thiel, Surf. Sci. **423**, 243 (1998).
[9] S. S. Kang, J. M. Dubois, and J. von Stebut, J. Mater. Res. **8**, 2471 (1993).
[10] C. Mancinelli, C. J. Jenks, P. A. Thiel, A. R. Ross, T. A. Lograsso, and A. J. Gellman, in *Quasicrystals*, edited by E. Belin-Ferré, P.A. Thiel, K. Urban, and A.-P. Tsai, MRS Symposia Proceedings No. 643 (Materials Research Society, Warrendale, NJ, 2001), pp. K8.2.1–K8.2.10.
[11] C. Mancinelli, C. J. Jenks, P. A. Thiel, and A. J. Gellman, J. Mater. Res. **18**, 1447 (2003).
[12] R. P. Matthews, C. I. Lang, and D. Shechtman, Tribol. Lett. **7**, 179 (2000).
[13] J. Y. Park, D. F. Ogletree, M. Salmeron, C. J. Jenks, and P. A. Thiel, Tribol. Lett. **17**, 629 (2004).
[14] J. Y. Park, D. F. Ogletree, M. Salmeron, R. A. Ribeiro, P. C. Canfield, C. J. Jenks, and P. A. Thiel, Phys. Rev. B **71**, 144203 (2005).
[15] D. M. Rampulla, C. M. Mancinelli, I. F. Brunell, and A. J. Gellman, Langmuir **21**, 4547 (2005).
[16] I. L. Singer, J. M. Dubois, J. M. Soro, D. Rouxel, and J. von Stebut, in *Proceedings of the 6th International Conference on Quasicrystals (ICQ6)*, edited by S. Takeuchi and T. Fujiwara (Singapore, 1998), pp. 769-772.
[17] J. von Stebut, C. Strobel, and J. M. Dubois, in *Proceedings of the Fifth International Conference on Quasicrystals (ICQ5)*, edited by C. Janot and R. Mosseri (Singapore, 1996), p. 704.
[18] J. von Stebut, J. M. Soro, P. Plaindoux, and J. M. Dubois, in *New Horizons in Quasicrystals Research and Applications*, edited by A. I. Goldman, D. J. Sordelet, P. A. Thiel, and J. M. Dubois (World Scientific Publishing, Singapore, 1997) p. 248.

[19] J. von Stebut, C. Comte, M. Zandona, J. M. Dubois, and D. Sordelet, in *Proceedings of the Sixth International Conference on Quasicrystals (ICQ6)*, edited by S. Takeuchi and T. Fujiwara (Singapore, 1998), pp. 777–781.
[20] L. Xiaodong, L. Zhang, and H. Gao, J. Phys. D **37**, 753 (2004).
[21] L.-M. Zhang, P. Brunet, H.-C. Zhang, C. Dong, and J.-M. Dubois, Tribol. Lett. **8**, 233 (2000).
[22] M. Enachescu, R. W. Carpick, D. F. Ogletree, and M. Salmeron, J. Appl. Phys. **95**, 7694 (2004).
[23] J. Y. Park, D. F. Ogletree, M. Salmeron, R. A. Ribeiro, P. C. Canfield, C. J. Jenks, and P. A. Thiel, Philos. Mag. **86**, 945 (2006).
[24] M. Dienwiebel, G. S. Verhoeven, N. Pradeep, J. W. M. Frenken, J. A. Heimberg, and H. W. Zandbergen, Phys. Rev. Lett. **92**, 126101 (2004).
[25] L. Howald, R. Luthi, E. Meyer, and H. J. Guntherodt, Phys. Rev. B **51**, 5484 (1995).
[26] J. Y. Park, D. F. Ogletree, M. Salmeron, R. A. Ribeiro, P. C. Canfield, C. J. Jenks, and P. A. Thiel, Science **309**, 1354 (2005).
[27] J. Y. Park, D. F. Ogletree, M. Salmeron, R. A. Ribeiro, P. C. Canfield, C. J. Jenks, and P. A. Thiel, Phys. Rev. B **72**, 220201(R) (2005).
[28] RHK Technology, Troy, MI, Model number UHV-350.
[29] J. Y. Park, R. J. Phaneuf, D. F. Ogletree, and M. Salmeron, Appl. Phys. Lett. **86**, 172105 (2005).
[30] J. Y. Park, G. M. Sacha, M. Enachescu, D. F. Ogletree, R. A. Ribeiro, P. C. Canfield, C. J. Jenks, P. A. Thiel, J. J. Saenz, and M. Salmeron, Phys. Rev. Lett. **95**, 136802 (2005).
[31] NT-MDT Co., Zelenograd Research Institute of Physical Problems, Moscow, Russia.
[32] J. E. Sader, J. W. M. Chon, and P. Mulvaney, Rev. Sci. Instrum. **70**, 3967 (1999).
[33] D. F. Ogletree, R. W. Carpick, and M. Salmeron, Rev. Sci. Instrum. **67**, 3298 (1996).
[34] E. Barrena, C. Ocal, and M. Salmeron, J. Chem. Phys. **113**, 2413 (2000).
[35] I. R. Fisher, M. J. Kramer, Z. Islam, A. R. Ross, A. Kracher, T. Wiener, M. J. Sailer, A. I. Goldman, and P. C. Canfield, Philos. Mag. A **79**, 425 (1999).
[36] E. J. Cox, J. Ledieu, R. McGrath, R. D. Diehl, C. J. Jenks, and I. Fisher, in *Quasicrystals-Preparation, Properties, and Applications*, edited by E. Belin-Ferre, P. A. Thiel, A. P. Tsai, and K. Urban, MRS Symposia Proceedings No. 643 (Materials Research Society, Pittsburgh, 2001), pp. K11.3.1–K11.3.6.
[37] W. Steurer, Z. Kristallogr. **219**, 391 (2004).
[38] R. W. Carpick, N. Agrait, D. F. Ogletree, and M. Salmeron, Langmuir **12**, 3334 (1996).
[39] B. V. Derjaguin, V. M. Muller, and Y. P. Toporov, J. Colloid Interface Sci. **53**, 314 (1975).
[40] M. Enachescu, R. J. A. vandenOetelaar, R. W. Carpick, D. F. Ogletree, C. F. J. Flipse, and M. Salmeron, Phys. Rev. Lett. **81**, 1877 (1998).
[41] K. L. Johnson, K. Kendall, and A. D. Roberts, Proc. R. Soc. London, Ser. A **324**, 301 (1971).
[42] R. W. Carpick, D. F. Ogletree, and M. Salmeron, J. Colloid Interface Sci. **211**, 395 (1999).
[43] M. Liley, D. Gourdon, D. Stamou, U. Meseth, T. M. Fischer, C. Lautz, H. Stahlberg, H. Vogel, N. A. Burnham, and C. Duschl, Science **280**, 273 (1998).
[44] R. W. Carpick, D. Y. Sasaki, and A. R. Burns, Tribol. Lett. **7**, 79 (1999).
[45] H. Bluhm, U. D. Schwarz, and K. P. Meyer, Appl. Phys. A: Mater. Sci. Process. **61**, 525 (1995).
[46] A. Ishizaka and Y. Shiraki, J. Electrochem. Soc. **133**, 666 (1986).
[47] J. Y. Park and R. J. Phaneuf, J. Vac. Sci. Technol. B **21**, 1254 (2003).
[48] R. W. Carpick and M. Salmeron, Chem. Rev. (Washington, D.C.) **97**, 1163 (1997).
[49] S.-L. Chang, J. W. Anderegg, and P. A. Thiel, J. Non-Cryst. Solids **195**, 95 (1996).
[50] P. J. Pinhero, J. W. Anderegg, D. J. Sordelet, M. F. Besser, and P. A. Thiel, Philos. Mag. B **79**, 91 (1999).
[51] J. S. Ko and A. J. Gellman, Langmuir **16**, 8343 (2000).
[52] M. Hirano, K. Shinjo, R. Kaneko, and Y. Murata, Phys. Rev. Lett. **67**, 2642 (1991).
[53] T. Gyalog and H. Thomas, Europhys. Lett. **37**, 195 (1997).
[54] G. He, M. H. Muser, and M. O. Robbins, Science **284**, 1650 (1999).
[55] M. Hirano, K. Shinjo, R. Kaneko, and Y. Murata, Phys. Rev. Lett. **78**, 1448 (1997).
[56] J. Ferrante and J. R. Smith, Surf. Sci. **38**, 77 (1973).
[57] A. Vanossi, J. Roder, A. R. Bishop, and V. Bortolani, Phys. Rev. E **63**, 017203 (2001).
[58] S. Martin, A. F. Hebard, A. R. Kortan, and F. A. Thiel, Phys. Rev. Lett. **67**, 719 (1991).
[59] D. L. Zhang, S. C. Cao, Y. P. Wang, L. Lu, X. M. Wang, X. L. Ma, and K. H. Kuo, Phys. Rev. Lett. **66**, 2778 (1991).
[60] J. A. Barrow, B. A. Cook, P. C. Canfield, and D. J. Sordelet, Phys. Rev. B **68**, 104202 (2003).
[61] E. Macia, Rep. Prog. Phys. **69**, 397 (2006).
[62] J. Hafner, M. Krajci, and M. Mihalkovic, Phys. Rev. Lett. **76**, 2738 (1996).
[63] W. Theis, H. R. Sharma, K. J. Franke, and K. H. Rieder, Prog. Surf. Sci. **75**, 227 (2004).